Method of obtaining optical sectioning by using structured light in a conventional microscope

M. A. A. Neil, R. Juškaitis, and T. Wilson

Department of Engineering Science, University of Oxford, Parks Road, Oxford OX1 3PJ, UK

Received August 26, 1997

We describe a simple method of obtaining optical sectioning in a conventional wide-field microscope by projecting a single-spatial-frequency grid pattern onto the object. Images taken at three spatial positions of the grid are processed in real time to produce optically sectioned images that are substantially similar to those obtained with confocal microscopes. © 1997 Optical Society of America

The confocal scanning optical microscope is a coherent image-formation system in which all spatial frequencies within the transfer function attenuate with defocus.[1,2] This means that only in-focus detail is imaged efficiently, which permits volume structures to be examined in three dimensions. The image formation in a conventional wide-field microscope, on the other hand, is in general partially coherent, and not all spatial frequencies within the transfer function attenuate with defocus; hence these systems do not possess the optical sectioning properties of the confocal instruments. However, if we examine the weak object transfer function for these instruments,[1] we find that it is only the zero spatial frequency that does not attenuate with defocus. This suggests the basis of our approach to obtain optically sectioned images from a conventional wide-field microscope. We modify the illumination system of the microscope to project a single-spatial-frequency grid pattern onto the object. The microscope will then image efficiently only that portion of the object where the grid pattern is in focus. We will thus obtain an optically sectioned image of the object but with the unwanted grid pattern superimposed. The rate of attenuation with defocus or optical sectioning strength will, of course, depend on the particular spatial frequency that is projected onto the object. The ideal of projecting various patterns onto an object to obtain information about their three-dimensional structure is not new, and various methods for doing this have been suggested.[3,4] The fundamental problem with all these approaches in that to be useful a simple method must be available to remove the unwanted grid pattern from the optically sectioned image. The approaches to microscopy with which we are familiar[3,4] all involve the use of some form of matched detector grid that must be aligned to within stringent requirements. It therefore seems unlikely that these approaches will lead to rugged, easily implementable designs. In this Letter we present a simple method to remove the grid pattern that permits us to obtain optically sectioned images from a conventional microscope in real time.

The optical system consists simply of an illumination mask $S(t_0, w_0)$, which is imaged onto an object of amplitude transmittance or reflectance $\tau(t_1, w_1)$. The final image is recorded by a CCD camera in the image plane (t, w). The mask is illuminated incoherently, which permits us to write the image intensity as

$$I(t, w) = \iint S(t_0, w_0) \left| \iint h_1(t_0 + t_1, w_0 + w_1) \times \tau(t_1, w_1) h_2(t_1 + t, w_1 + w) \mathrm{d}t_1 \mathrm{d}w_1 \right|^2 \mathrm{d}t_0 \mathrm{d}w_0 , \quad (1)$$

where $h_{1,2}$ represents the amplitude point-spread functions of the two lenses. We also elect to work in optical coordinates (t, w) that are related to real coordinates (x, y) through $(t, w) = (2\pi/\lambda)(x, y)n \sin \alpha$, where $n \sin \alpha$ is the numerical aperture (NA) and λ denotes the wavelength.[1,2]

Let us now assume that the illumination mask takes the form of a one-dimensional grid, which we can write for simplicity as

$$S(t_0, w_0) = 1 + m \cos(\tilde{\nu} t_0 + \phi_0) , \quad (2)$$

where m denotes a modulation depth and ϕ_0 is an arbitrary spatial phase. The normalized spatial frequency $\tilde{\nu}$ is related to the actual spatial frequency ν through $\tilde{\nu} = \beta\lambda\nu/\mathrm{NA}$, where β denotes the magnification between the grid plane and the specimen plane. If we now substitute Eq. (2) into Eq. (1) we have

$$I(t, w) = I_0 + I_c \cos \phi_0 + I_s \sin \phi_0 , \quad (3)$$

where I_0 is given by Eq. (1) with $S = 1$ and, of course, represents a conventional wide-field image. I_c and I_s represent the images that are due to masks of forms $m \cos(\tilde{\nu} t_0)$ and $m \sin(\tilde{\nu} t_0)$, respectively. These definitions suggest that if we are able to form $I_p = (I_c^2 + I_s^2)^{1/2}$ we would remove the grid pattern from the image of the specimen. We can readily achieve this result by taking three images, I_1, I_2, and I_3, which correspond to the relative spatial phases $\phi_0 = 0$, $\phi_0 = 2\pi/3$, and $\phi_0 = 4\pi/3$, respectively. We can thus obtain an optically sectioned image, which does not contain I_0, by calculating

$$I_p = \left[(I_1 - I_2)^2 + (I_1 - I_3)^2 + (I_2 - I_3)^2 \right]^{1/2} , \quad (4)$$

which is analogous to square-law detection in communications systems.[5] Alternatively, I_p can be formed as

$$I_p = \left| I_1 + I_2 \exp j\frac{2\pi}{3} + I_3 \exp \frac{4\pi}{3} \right| , \quad (5)$$

0146-9592/97/241905-03$10.00/0

which is the equivalent of homodyne detection. We note that the conventional image, I_0, can be recovered from $I_1 + I_2 + I_3$.

To confirm that the image obtained in this way does possess an optical sectioning property in the sense usually understood in confocal microscopy we consider how the image intensity decays with defocus when a plane minor is used as a specimen. We set $\tau(t_0, w_0) = 1$ in Eq. (1), which together with Eq. (3)–(5) permits us to write

$$I_p(t, w) = \left| \iint \exp \tilde{\nu} t_0 \left| \iint h_1(t_0 + t_1, w_0 + w_1) \times h_2(t_1 + t, w_1 + w) \mathrm{d}t_1 \mathrm{d}w \right|^2 \mathrm{d}t_0 \mathrm{d}w_0 \right| . \quad (6)$$

It is then a simple matter to introduce the pupil functions $P_{1,2}(\xi, \eta)$ through the Fourier transform of the amplitude point-spread functions, $h_{1,2}(t, w)$, to give

$$I_p = \left| \iint P_1(\xi, \eta) P_2(\xi, \eta) P_1^*(\xi - \tilde{\nu}, \eta) \times P_2^*(\xi - \tilde{\nu}, \eta) \mathrm{d}\xi \mathrm{d}\eta \right| , \quad (7)$$

which, for the case of equal pupil functions $P_1 = P_2$, can be written, in the presence of defocus u, as

$$I_p(u) = |g(2u, \tilde{\nu})| , \quad (8)$$

where $g(u, \tilde{\nu}) = P \otimes P^*$, where $\otimes$ denotes the convolution operation and the normalized defocus parameter u is related to the actual defocus z through $u = 8(\pi/\lambda) z \sin^2(\alpha/2)$.

We note that the function $g(u, \tilde{\nu})$ is formally identical to the weak object transfer function in a conventional microscope. That function can readily be evaluated numerically, but it will suffice for our purposes to use an approximation that is due to Stokseth,[6] which permits us to write

$$g(u, \tilde{\nu}) = f(\tilde{\nu}) \left\{ 2 \frac{J_1[u\tilde{\nu}(1 - \tilde{\nu}/2)]}{[u\tilde{\nu}(1 - \tilde{\nu}/2)]} \right\} , \quad (9)$$

with $f(\tilde{\nu}) = 1 - 0.69\tilde{\nu} + 0.0076\tilde{\nu}^2 + 0.043\tilde{\nu}^3$. We therefore find that

$$I_p(u) \sim \left| 2 \frac{J_1[2u\tilde{\nu}(1 - \tilde{\nu}/2)]}{[2u\tilde{\nu}(1 - \tilde{\nu}/2)]} \right| , \quad (10)$$

which confirms that our instrument does exhibit optical sectioning in the same fashion as a confocal microscope. The strength of the sectioning does, of course, depend on the value of $\tilde{\nu}$ chosen. We note that in the limit of $\tilde{\nu} = 0$, which corresponds to removing the grid pattern, $I_s(u) =$ constant, as would be expected in the conventional microscope limit. The maximum sectioning strength is found to correspond to a normalized spatial frequency $\tilde{\nu} = 1$.

To demonstrate the ability of our system to produce optically sectioned images in real time we introduce a 40-line/mm one-dimensional grid into the illumination path of a conventional microscope. As we used infinity tube length optics, it was necessary to introduce separate lenses both to project the image of the grid onto the specimen and to image the specimen onto the CCD camera. The result was an effective magnification between the illumination plane and the specimen of $(50/180)M$, where M is the nominal magnification of the objective lens. A 15-W tungsten-halogen lamp was used as the light source, together with a green filter (bandwidth 100 nm). Images were recorded with a CCD camera and transferred to a Matrox Meteor frame grabber. The grid was moved in a simple saw-tooth fashion synchronized to the camera frame rate such that any three successive camera images corresponded to a spatial shift of one third of a period in the position of the projected image of the grid (Fig. 1). The fact that the grid is in motion during the integration time of each frame results in a reduction in the values of I_c and I_s in Eq. (3) by a factor of $\mathrm{sinc}(\pi t/3T)$, where t is the integration time of the camera and T is the time between the recording of successive frames. In our case $T = 2t = 40$ ms, and hence this factor is only 0.955. In the worst case, $T = t$, the factor falls to only 0.827. The optically sectioned images were obtained by use of Eq. (4) together with a look-up table that mapped all possible combinations of I_1, I_2, and I_3 from our 8-bit camera to I_p.

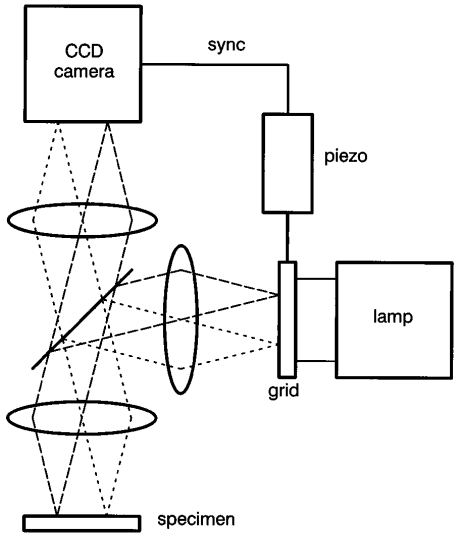

Fig. 1. Schematic of the optical arrangement.

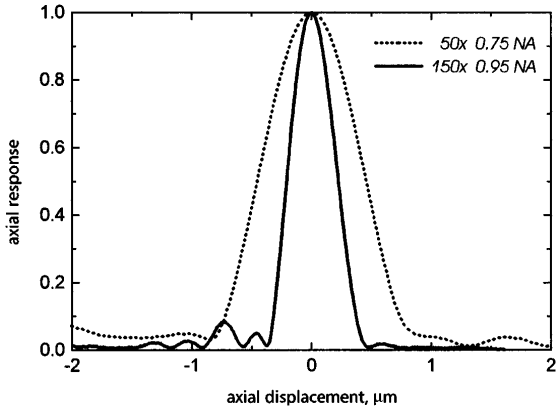

Fig. 2. Measured axial responses of the system.

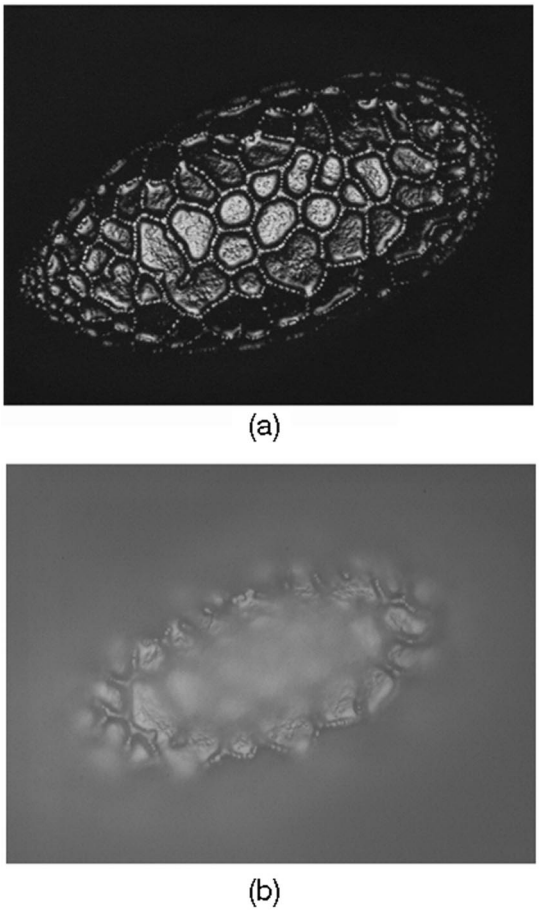

Fig. 3. (a) Autofocus image of lily pollen grain. The field size is 100 μm $\times$ 70 μm. (b) Conventional image of the lily pollen grain when the microscope is focused in a mid-depth plane.

To measure the optical sectioning strength of our microscope we used a plane mirror together with a calibrated axial translation stage; the resulting axial responses are shown in Fig. 2 for two Olympus MD Plan objectives. We note that the use of the 50×, 0.75 NA corresponds to $\tilde{\nu} = 0.4$ in our system, for which relation (10) predicts a FWHM of 0.87 μm, which compares well with the measured value of 0.91 μm. Theory predicts that the 150×, 0.95 NA dry objective should give $\tilde{\nu} = 0.8$ and hence a FWHM of 0.27 μm. In practice, we measured 0.43 μm, which corresponds to a numerical aperture of this lens of 0.85 rather than 0.95. This discrepancy is consistent with other measurements performed with high-aperture lenses[7] and may be due to a variety of causes, one of which is likely to be the strong attenuation of the marginal rays that leads to an effective apodization of the pupil function.

Finally, in Fig. 3 we show images obtained by imaging the thick volume structure of a lily pollen grain. Figure 3(a) represents an autofocus image obtained by displaying the maximum image intensity at each pixel throughout a 30-μm axial scan with the 50×, 0.75 NA objective lens. The full surface texture of the grain is well resolved over the entire image volume. Figure 3(b), on the other hand, shows a conventional image taken at a plane midway through the grain. It is clear that a good deal of out-of-focus blur is present here, which prevents any meaningful three-dimensional image processing from being carried out.

In conclusion, we have presented an extremely simple modification to a conventional microscope illumination system that permits optically sectioned images to be obtained and hence volume rendering of thick objects to be carried out. The image formation is formally different from that obtained in a confocal microscope, and the transfer function is found to be slightly different for object features that vary in the t and w directions. However, the differences are not great, and in all the specimens that we examined with this simple technique we obtained images that were substantially similar to those obtained with laser-based confocal systems.

This research was funded by the Paul Instrument Fund of the Royal Society.

References

1. T. Wilson and C. J. R. Sheppard, *Theory and Practice of Scanning Optical Microscopy* (Academic, London, 1984).
2. T. Wilson, ed., *Confocal Microscopy* (Academic, London, 1990).
3. B. Neumann, Proc. SPIE **1139,** 102 (1989).
4. C. G. Morgan, "Optical sensor for imaging an object," U.S. patent 5,381,236 (January 10, 1995).
5. A. B. Carlson, *Communication Systems* (McGraw-Hill, New York, 1988).
6. P. A. Stokseth, J. Opt. Soc. Am. **59,** 1314 (1969).
7. T. Wilson and R. Juškaitis, Bioimaging **3,** 35 (1995).